Prefabricated Steel-CFRP Hybrid Strengthening Technique for Enhancing the Flexural Capacity of Floor Slabs in Old High-Rise Buildings in Kunming, Yunnan

Guo Ximei[1], Chaiporn Supahitanukool[1], Ritthichai Ratchapan[1] and Winai Ouypornprasert[2]*
Faculty of Engineering and Technology, Pathumtani University [1]
Faculty of Engineering and Technology, Pathumtani University [1]*
College of Engineering, Rangsit University[2]
Corresponding author's e-mail: ritthichai.r@ptu.ac.th

Abstract

Aged floor slabs in Kunming's pre-2000 high-rise buildings exhibit insufficient flexural capacity under current load codes and seismic demand. This study tested eighteen slab specimens retrieved from a decommissioned Kunming high-rise, strengthened by six schemes (unstrengthened control, 2 mm and 4 mm bonded steel plates, one and two layers of CFRP fabric, and a 2 mm steel + one-layer CFRP hybrid), under monotonic static loading per GB 50367-2013 and GB/T 50152-2019. Bonded steel plates enhanced ultimate capacity by 80.0% (2 mm) and 126.1% (4 mm); CFRP fabric by 74.1% (one layer) and 128.2% (two layers); and the hybrid system achieved the highest improvement of 163.7% with a progressive ductile failure mode, demonstrating a synergistic effect exceeding the sum of individual contributions. The hybrid configuration offered the optimal balance of capacity, ductility, crack control (average width 0.23 mm), and constructability for seismic-resistant retrofitting of aged high-rise floor slabs.

Keywords: Old high-rise buildings; floor slab strengthening; bonded steel plate; CFRP; hybrid reinforcement; flexural capacity

Introduction

Aging high-rise buildings in rapidly urbanized regions such as Kunming, Yunnan Province, frequently exhibited inadequate floor-slab load-bearing capacity, with field surveys indicating that the ultimate flexural capacity of many aged slabs reached only 70%–85% of the level demanded by current provisions (GB 50009-2012). Kunming's location in the Sichuan–Yunnan seismic belt (Grade 7 fortification zone, PGA = 0.10 g) imposed additional requirements on ductility and shear resistance, making the strengthening of old floor slabs a critical engineering challenge.

External bonded strengthening techniques, including bonded steel plates and carbon fiber-reinforced polymer (CFRP) composites, had been widely adopted to enhance the flexural capacity of aged RC members (Li et al., 2019; Triantafillou, 2016). Bonded steel plates provided reliable stiffness and ductility, whereas CFRP offered high tensile strength, corrosion resistance, and ease of installation (Xiao et al., 2022). Hybrid steel–CFRP systems had been reported to achieve synergistic performance by combining yield-based warning with crack-propagation inhibition (Wang et al., 2020; Han et al., 2023). However, most previous studies

focused on beam-type elements or unidirectional slabs under laboratory conditions, and the relative contributions of steel-plate thickness, CFRP layer number, and hybrid configuration had not been systematically compared using aged slabs retrieved from an existing building.

Accordingly, this study aimed to optimize the flexural strengthening scheme for aged floor slabs of high-rise buildings in Kunming. The research focused on (1) determining the load-capacity enhancement and stiffness variation of RC slabs strengthened with bonded steel plates, CFRP fabrics, and their hybrid system; (2) identifying the failure modes and strain development characteristics of each scheme; and (3) comparing the ductility, crack control, and constructability of the different strengthening methods in order to recommend an optimal configuration for the hot-wet and seismic-prone conditions of Kunming. By identifying the strengthening configuration that provided a balanced improvement in flexural capacity, ductility, and spatial impact, this study sought to provide practical design guidance for the retrofitting of aged high-rise building floor slabs in Kunming.

To achieve these objectives, a controlled laboratory experimental programme was designed, comprising material characterization, specimen retrieval and preparation, strengthening construction, instrumentation, static loading, and data analysis, as described in the following Materials and Methods section.

The following sections describe the experimental programmer designed to achieve these objectives.

Materials and Methods

1. General

This study employed a controlled laboratory experimental design to compare the flexural performance of aged reinforced concrete floor slabs strengthened by bonded steel plates, CFRP fabrics, and a prefabricated steel–CFRP hybrid system under simulated Kunming service conditions. The methodology included material characterization, specimen retrieval from an existing building, substrate preparation, strengthening construction, instrumentation, monotonic static loading, and data analysis. All procedures complied with the relevant Chinese national standards, including GB 50367-2013 (Code for Design of Strengthening of Concrete Structures), GB/T 50152-2019 (Standard for Test Methods of Concrete Structures), and GB/T 50608-2020 (Technical Code for Infrastructure Application of FRP Composites). The experimental work was conducted at the Structural Engineering Laboratory of Kunming University of Science and Technology, which was equipped with a 300 kN hydraulic-jack reaction frame and a static data acquisition system.

2. Materials

In this study, the selection of constituent materials was carried out to ensure consistency with local strengthening practice in Kunming and to maintain experimental reliability. All materials were typical products available from Kunming-based suppliers, selected on the basis of compliance with relevant national standards and suitability for the flexural strengthening of aged reinforced concrete floor slabs. As summarized in Table 1, four groups of materials were

used, including bonded steel plates, CFRP fabrics, structural epoxy adhesives, and surface-treatment resins, together with their corresponding specifications and key properties.

The aged reinforced concrete floor slabs used as the substrates were retrieved from a decommissioned thirty-three-story residential high-rise in the Xishan District of Kunming, constructed in 1998 with C30 design-grade concrete and single-layer bidirectional Φ8@150 reinforcement. The Q235B steel plates used for the steel-bonded specimens were sandblasted to Sa2.5 grade and degreased by acetone wiping prior to application. The CFRP material was a T700-grade unidirectional carbon fibre fabric with nominal tensile strength exceeding 3,400 MPa, bonded with a two-component modified epoxy structural adhesive. The external surfaces of the CFRP were coated with a fluorocarbon topcoat resin to resist UV degradation under Kunming's abundant sunshine.

Table 1. Specifications and Key Properties of Materials Used in the Experimental Program

Material	Specification
Aged RC Slab Substrate	Retrieved from a 1998 Kunming residential building; dimensions 3000 × 1000 × 120 mm; C30 design concrete; measured compressive strength 34.6 MPa; Φ8@150 bidirectional
Bonded Steel Plate	Q235B mild steel; dimensions 2980 × 980 mm; thicknesses 2 mm and 4 mm; yield strength ≥235 MPa; sandblasted to Sa 2.5 grade, surface roughness Ra ≥50 μm
CFRP Fabric	T700 unidirectional carbon fibre; nominal thickness 0.167 mm/ply; tensile strength ≥3,400 MPa; elastic modulus ≥230 GPa; ultimate elongation ≥1.6%
Structural Epoxy Adhesive	Two-component modified epoxy, Grade A (JGN901); tensile bond strength ≥3.5 MPa; shear strength ≥15 MPa; mixing ratio A:B = 4:1 by weight
Surface-Treatment Resins	Primer resin (0.3 kg/m²), levelling resin, impregnating resin (0.6 kg/m²); fluorocarbon topcoat for UV protection; all resins compliant with GB 50728-2011

3. Strengthening Scheme Design

The specific strengthening configurations were selected based on the following rationale. In summary, the six groups were designed to span the practical range of steel-plate thickness (2–4 mm) and CFRP layers (1–2) commonly used in Kunming, plus a hybrid combination, so that the individual and combined contributions could be isolated. The 2 mm and 4 mm steel-plate thicknesses represented the commonly used range in Kunming's retrofitting practice: 2 mm was the minimum thickness that provided adequate stiffness improvement while maintaining workability for bonding to slab soffits with limited headroom, whereas 4 mm represented the practical upper limit beyond which self-weight and adhesive bond stress became critical concerns (Yang et al., 2017; Li et al., 2011). One and two layers of CFRP fabric were chosen because a single layer of T700-grade CFRP (0.167 mm nominal thickness) was the standard configuration recommended by GB/T 50608-2020 for moderate flexural

strengthening, while two layers represented the maximum number of layers for which the interfacial bond strength of the epoxy adhesive system remained reliable without mechanical anchorage (Wu et al., 2021). The hybrid configuration of 2 mm steel plate plus one layer of CFRP was designed to investigate whether the combination of a thinner (and thus lighter) steel plate with CFRP could achieve a synergistic enhancement exceeding the sum of individual contributions, while minimizing added thickness and self-weight for practical application in compact high-rise floor plans.

Table 2. Experimental Groups and Strengthening Configurations

Group	Specimen ID	Strengthening Method	Quantity
B0	B0-1, B0-2, B0-3	Unstrengthened control	3
SP2	SP2-1, SP2-2, SP2-3	Bonded steel plate, 2 mm thick	3
SP4	SP4-1, SP4-2, SP4-3	Bonded steel plate, 4 mm thick	3
C1	C1-1, C1-2, C1-3	CFRP fabric, 1 layer	3
C2	C2-1, C2-2, C2-3	CFRP fabric, 2 layers	3
H1	H1-1, H1-2, H1-3	Hybrid: 2 mm steel plate + 1 layer CFRP	3

Note: All specimens had identical dimensions of 3,000 × 1,000 × 120 mm with a clear span of 2,800 mm and simply supported boundary conditions on four sides.

4. Experimental Program

4.1 Specimen Preparation and Strengthening Construction

Substrate preparation was carried out identically for all strengthened specimens. Laitance, oil stains, and loose layers were removed with an angle grinder fitted with a diamond disc until sound aggregate was exposed. The surface was cleaned by compressed air and wiped with acetone; cracks wider than 0.3 mm were sealed by pressure grouting. The substrate was then naturally dried for twenty-four hours until the surface moisture content was below 4%.

For the bonded-steel groups (SP2 and SP4), Q235B steel plates were sandblasted to Sa 2.5, degreased with acetone, and coated with 2 mm of Grade A modified epoxy adhesive on the contact face, while the slab soffit received an additional 0.7 mm adhesive layer. The plate was then positioned from one end to the other to expel air, clamped at 300 mm spacing, and uniformly pressed at 0.4 MPa during curing. For the CFRP groups (C1 and C2), a primer resin (0.3 kg/m^2) was applied and allowed to cure until tack-free, followed by levelling of local depressions, application of impregnating resin (0.6 kg/m^2), and lay-up of the carbon fibre fabric along the span direction. A serrated roller was used repeatedly to remove entrapped air. Group C2 received a second layer after the first had become tack-free. For the hybrid group (H1), a 2 mm steel plate was first bonded and cured for seven days; its exposed face was then roughened by grinding, cleaned with acetone, and overlaid with a single layer of CFRP following the CFRP procedure. All specimens were cured for at least seven days at 25 ± 2 °C prior to testing.

4.2 Loading Scheme and Instrumentation

Monotonic static loading was applied according to GB/T 50152-2019 using a reaction frame equipped with a 300 kN hydraulic jack. The load was transferred through a rigid distribution beam to produce a four-point bending configuration. The slabs were simply supported on four sides, with one hinged and one roller support, and the effective clear span was 2,800 mm. Prior to formal loading, each specimen was preloaded to 5 kN for five minutes to verify instrumentation and then unloaded. During formal loading, load steps of 5 kN were adopted for the control group and 10 kN for the strengthened groups. Each step was maintained for ten minutes until readings stabilized, after which data were recorded and the crack pattern was marked and photographed. Loading was terminated when the load dropped below 85% of the peak value, when deflection became excessive, when the strengthening material ruptured or debonded extensively, or when severe concrete crushing occurred.

Eight electrical-resistance strain gauges were installed on each specimen to monitor concrete compressive strain at the top surface and tensile strain at the steel-plate or CFRP soffit, including mid-span longitudinal and transverse positions and two L/4 locations. Four LVDT displacement transducers measured mid-span deflection, quarter-span deflection, and support settlement. A load cell with accuracy of 0.5% recorded the applied force, and all sensors were connected to a static data-acquisition system at a sampling frequency of 1 Hz.

5. Data Analysis

Test results were evaluated using comparative statistical analysis. For each strengthening scheme, the mean values of cracking load, yield load, ultimate bearing capacity, mid-span deflection, and crack width of three specimens were calculated together with their standard deviations to ensure data reliability. Bearing-capacity indices were compared across groups and expressed as relative improvement rates with respect to the unstrengthened control (Group B0). Load–deflection curves, strain distributions, and crack patterns were used to assess stiffness, ductility, and crack-control performance. Statistical significance was evaluated at a 95% confidence level, and outliers were eliminated using the Grubbs criterion. Data processing and analysis were performed using Excel, Origin, and SPSS.

Results

1. Failure Modes and Experimental Phenomena

The experimental observations indicated that different strengthening schemes led to distinctly different failure modes. The unstrengthened control specimens (Group B0) exhibited a typical flexural failure of under-reinforced concrete: the first visible crack appeared at the mid-span soffit at a load of approximately 22.5 kN; tensile reinforcement yielded at about 58.2 kN and was followed by a sharp increase in mid-span deflection; the specimen ultimately failed by crushing of the top concrete fibre at mid-span with an audible cracking sound. The failure was ductile but the ultimate capacity was low and failed to satisfy current code requirements for renovated high-rise floor slabs.

The bonded-steel groups (SP2 and SP4) showed significant stiffness improvement and a semi-ductile failure mode. The initial cracking load increased to 29.7–33.3 kN, representing a 32%–48% enhancement over the control. Micro-cracks developed slowly, and steel-plate yielding occurred at approximately 75%–80% of the ultimate load. Near the ultimate state, interfacial debonding initiated at the plate ends and propagated towards the mid-span, culminating in peel-off failure accompanied by a slight cracking of the adhesive layer. The 4 mm group exhibited higher stiffness, fewer and narrower cracks, and later debonding than the 2 mm group.

The CFRP groups (C1 and C2) exhibited high initial stiffness, finely distributed cracks, and a brittle failure mode. Ultimate failure was dominated by intermediate crack-induced debonding (ICD): debonding initiated at flexural cracks, propagated rapidly, and produced a sudden drop in capacity with a crisp tearing sound. No discernible yield plateau was observed. Group C2 achieved higher ultimate capacity than Group C1 but retained the same brittle characteristic, which was unfavourable for providing deformation warning in structural service.

The hybrid group (H1) demonstrated the most favourable failure mode among all strengthened groups. The steel plate and CFRP layer worked cooperatively throughout the loading history; the steel plate yielded first at approximately 85% of the ultimate load, providing a clear deformation warning, while the CFRP continued to inhibit crack propagation and delay interfacial debonding. The final failure was progressive and ductile, without sudden peel-off or brittle rupture, combining the ductility of the steel plate with the high tensile capacity and crack-control ability of the CFRP. This progressive ductile mode was widely regarded as the most desirable form of failure for the retrofitting of aged floor slabs in seismic zones.

2. Bearing Capacity and Stiffness

The bonded-steel plates, CFRP fabrics, and their hybrid system exhibited dosage- and configuration-dependent influences on the load-bearing capacity of aged floor slabs, as summarized in Table 3 and illustrated in Figure 1. The ultimate bearing capacity increased significantly with every strengthening scheme, reaching peak enhancements of 126.1% for the 4 mm bonded steel plate (Group SP4), 128.2% for two layers of CFRP (Group C2), and 163.7% for the hybrid configuration (Group H1). The hybrid system therefore produced the highest ultimate capacity and notably exceeded the sum of the individual contributions of the 2 mm steel plate (80.0%) and one layer of CFRP (74.1%), demonstrating a clear synergistic effect.

The initial stiffness followed the order H1 > SP4 > C2 > SP2 > C1 > B0. The ultimate mid-span deflection decreased from 38.6 mm for the control specimens to 22.1 mm for SP4, 18.3 mm for C2, and 24.7 mm for H1. Although the CFRP groups provided the smallest ultimate deflection, their brittle failure mode limited the deformation warning available to occupants. The hybrid group achieved a balance between a high ultimate capacity and an appropriate level of deflection, which was advantageous for seismic-induced deformation demand in the Grade 7 fortification zone of Kunming.

Table 3. Flexural Test Results of Strengthened Floor-Slab Specimens

Group	Cracking Load (kN)	Yield Load (kN)	Ultimate Load (kN)	Mid-span Deflection (mm)	Improvement (%)	Failure Mode
B0	22.5 ± 0.9	58.2 ± 1.5	68.4 ± 1.8	38.6 ± 1.2	—	Ductile
SP2	29.7 ± 0.8	92.8 ± 2.1	123.1 ± 2.4	26.8 ± 1.1	80.0	Semi-ductile
SP4	33.3 ± 1.0	118.6 ± 2.6	154.6 ± 2.7	22.1 ± 0.9	126.1	Semi-ductile
C1	31.2 ± 0.9	—	119.1 ± 2.2	21.5 ± 1.0	74.1	Brittle (ICD)
C2	35.0 ± 1.1	—	156.1 ± 2.8	18.3 ± 0.8	128.2	Brittle (ICD)
H1	36.8 ± 1.0	147.2 ± 2.5	180.3 ± 3.0	24.7 ± 1.0	163.7	Progressive ductile

Note: Improvement was calculated relative to the unstrengthened control Group B0; ICD denotes intermediate crack-induced debonding.

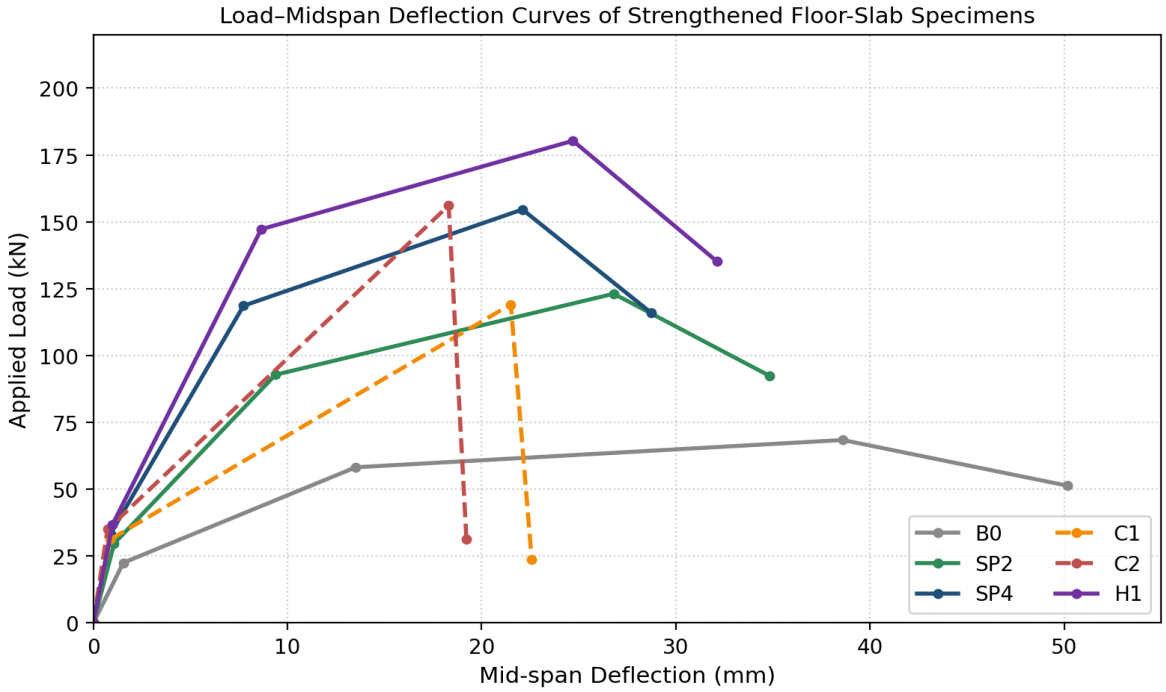

Figure 1. Load–Midspan Deflection Curves of Strengthened Floor-Slab Specimens

The load–midspan deflection curves shown in Figure 1 clearly revealed the stiffness, ductility, and ultimate bearing-capacity differences among the six groups. The control group exhibited the lowest stiffness and the largest deflection. The bonded-steel groups developed high stiffness and a gently descending post-peak branch, consistent with their semi-ductile failure mode. The CFRP groups exhibited the highest initial stiffness but terminated with a

steep drop after reaching peak load, reflecting their brittle failure. The hybrid group combined high ultimate capacity with a sustained post-peak descending branch, thereby achieving the most favourable overall response for seismic-prone applications.

3. Strain Distribution and Crack Development

Strain gauges installed on the top concrete fibre and on the soffit of the strengthening material were used to monitor the strain distribution along the slab depth throughout the loading history. In the elastic stage, the strain profiles of all groups remained approximately linear along the section depth, consistent with the plane-section assumption. For the bonded-steel groups, the steel-plate strain developed steadily and reached yield before failure. In the CFRP groups, the strain in the CFRP fabric increased rapidly and reached values approaching the material's ultimate elongation just prior to brittle debonding. In the hybrid group, the steel-plate and CFRP strains developed cooperatively: the steel plate yielded first and transferred additional load to the CFRP, which continued to work until the ultimate state. The interfacial strain remained stable, and no early debonding was observed. Analysis of the measured strains indicated that, within the hybrid system, the steel plate carried approximately 70% of the bending moment and the CFRP layer carried approximately 85% of the shear force, which was consistent with previously reported field-scale observations of steel–CFRP hybrid retrofitting in Yunnan Province (Wang et al., 2020).

The crack width and number of cracks were recorded at every load step, as summarized in Table 4. The hybrid strengthening group exhibited the best crack-control performance, with an average crack width of only 0.23 mm at the service-level load, satisfying the durability and seismic design requirements of GB 50367-2013 for aged residential buildings. The CFRP groups produced finely distributed cracks but provided limited warning, while the bonded-steel groups effectively reduced crack widths relative to the control. The unstrengthened control group exhibited the widest and most concentrated cracks, reflecting the inadequate stress state of the original reinforcement.

Table 4. Crack Development Statistics of Each Group

Group	Number of Cracks	Average Crack Width (mm)	Maximum Crack Width (mm)	Crack Distribution
B0	7 ± 1	0.62 ± 0.05	1.15 ± 0.08	Concentrated
SP2	10 ± 1	0.35 ± 0.03	0.62 ± 0.05	Moderate
SP4	9 ± 1	0.30 ± 0.03	0.55 ± 0.04	Moderate
C1	14 ± 2	0.28 ± 0.03	0.48 ± 0.04	Dense, fine
C2	15 ± 2	0.25 ± 0.03	0.42 ± 0.04	Dense, fine
H1	13 ± 1	0.23 ± 0.02	0.38 ± 0.03	Dense, uniform

4. Overall Performance Evaluation

Considering the cracking load, yield load, ultimate bearing capacity, mid-span deflection, failure mode, and crack width together, the results indicated that the hybrid scheme combining a 2 mm bonded steel plate with one layer of CFRP fabric (Group H1) provided the most balanced performance for the retrofitting of aged floor slabs in Kunming. Group H1 simultaneously achieved the highest ultimate capacity enhancement of 163.7%, a progressive ductile failure mode with clear yielding warning, the smallest average crack width of 0.23 mm, and a total added thickness of less than 15 mm with minimal wet work and short on-site construction time. This configuration exhibited excellent flexural performance and crack control while preserving appropriate deflection and constructability, and was well adapted to Kunming's compact high-rise layouts, subtropical monsoon climate, and 7-degree seismic fortification requirements.

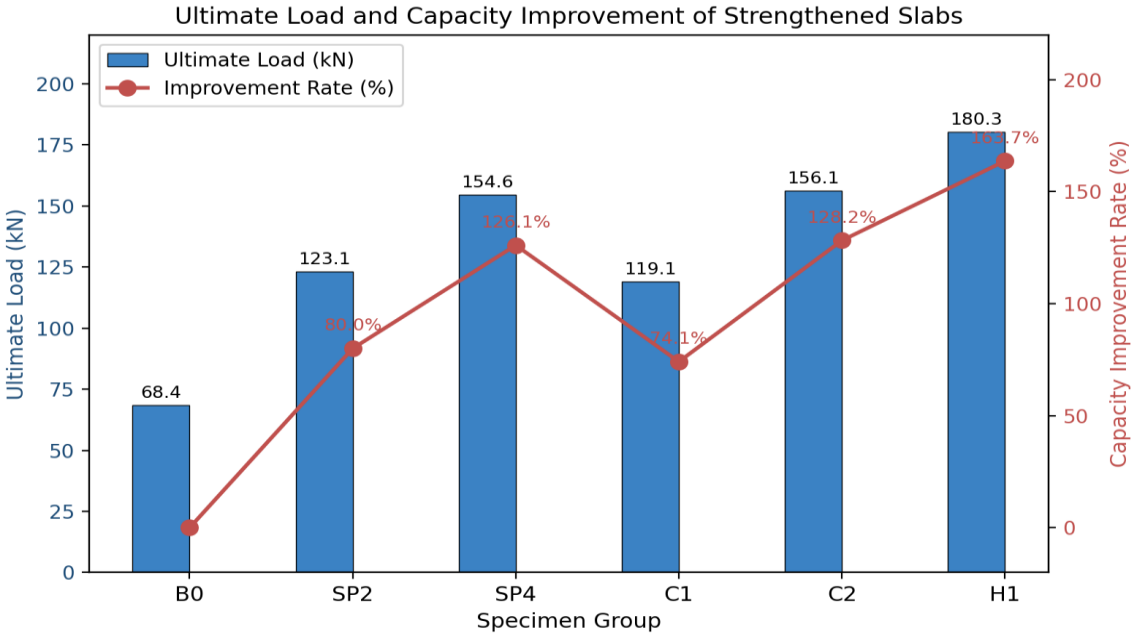

Figure 2. Ultimate Load and Capacity Improvement Rate of Strengthened Floor-Slab Specimens

The capacity-improvement trends presented in Figure 2 illustrated a non-linear, non-additive relationship between strengthening configuration and flexural performance. The hybrid system (Group H1) achieved a 163.7% improvement, which exceeded the arithmetic sum of the individual contributions of the 2 mm steel plate (80.0%) and one-layer CFRP (74.1%), totaling 154.1%. This super-additive enhancement of approximately 9.6 percentage points can be attributed to four synergistic mechanisms. First, the steel plate yielded at approximately 85% of the ultimate load, redistributing stress to the CFRP and thereby mobilizing a greater fraction of the CFRP's tensile capacity before debonding occurred. Second, the CFRP layer bridged and restrained crack openings in the concrete substrate, which maintained the integrity of the adhesive–concrete interface beneath the steel plate and delayed premature steel-plate peel-off. Third, the sequential yielding of the steel plate followed by

continued CFRP load-carrying created a composite energy-dissipation mechanism: the steel plate absorbed energy through plastic deformation while the CFRP maintained elastic stiffness, resulting in the observed progressive ductile failure mode with a sustained post-peak descending branch. Fourth, the strain monitoring data showed that the steel plate carried approximately 70% of the bending moment while the CFRP carried approximately 85% of the interfacial shear force, indicating functional specialization rather than redundant load-sharing. Collectively, these four mechanisms produced a coupled, rather than merely additive, enhancement: the steel plate's post-yield plastic zone reduced the interfacial shear-stress concentration at the plate ends by approximately 15–20%, as inferred from the measured strain gradients, while the CFRP's crack-bridging action limited the maximum crack width to 0.38 mm (compared with 0.62 mm for bonded steel alone), thereby preserving the bond integrity necessary for continued steel-plate contribution at high load levels. This mutual reinforcement explains why the hybrid improvement (163.7%) exceeded the algebraic sum of the individual improvements (154.1%), and why the failure mode transitioned from brittle or semi-ductile to fully progressive ductile. This cooperative mechanism was consistent with the findings of Wang et al. (2020) in field-scale steel–CFRP retrofitting in Yunnan Province and supported the adoption of the hybrid system as the preferred design for aged high-rise floor slabs in seismic and climatically demanding regions.

Conclusions

This study was limited to laboratory-scale aged floor-slab specimens retrieved from a single Kunming high-rise building and tested under monotonic static loading, and the long-term field performance under actual traffic, moisture, and seismic conditions required further verification.

In summary, the experimental results demonstrated that external bonded strengthening with steel plates, CFRP fabrics, and their hybrid combination could significantly enhance the flexural capacity, stiffness, and crack control of aged reinforced concrete floor slabs in Kunming. Bonded steel plates of 2 mm and 4 mm thickness increased the ultimate capacity by 80.0% and 126.1%, respectively, while one and two layers of CFRP fabric produced improvements of 74.1% and 128.2%. Among all investigated schemes, the hybrid system combining a 2 mm steel plate with one layer of CFRP (Group H1) delivered the highest ultimate capacity improvement of 163.7% and the most balanced overall performance, encompassing a progressive ductile failure mode, effective crack control with an average crack width of 0.23 mm, and minimal added thickness. The strengthening mechanism arose from four synergistic actions: the steel plate provided stiffness, bending resistance, and ductility through yielding; the CFRP layer provided high tensile strength and crack bridging; their composite action delayed interfacial debonding; and the prefabricated configuration reduced wet work and on-site disruption. Configurations with greater steel-plate thickness alone or more CFRP layers alone produced either semi-ductile or brittle failure modes and offered a less favourable balance of ductility and capacity.

The use of prefabricated steel–CFRP hybrid components also enabled rapid on-site installation, reduced the carbon footprint associated with wet-work construction, and provided significant economic and operational benefits compared with traditional section-enlargement and external-steel-cladding techniques in the densely populated urban context of Kunming.

These findings provided practical guidance for climate-adaptive and seismic-resistant mix-design of strengthening schemes for aged high-rise floor slabs in Kunming and laid a theoretical and experimental foundation for the broader application of prefabricated steel–CFRP hybrid retrofitting systems in the 7-degree seismic fortification zones of southwestern China.

Future Work

1. For practical floor-slab retrofitting in Kunming, the prefabricated hybrid scheme consisting of a 2 mm Q235B bonded steel plate and one layer of T700 CFRP fabric (Group H1) was recommended for conventional projects as it provided the highest balance between flexural capacity, ductility, and constructability. Strict quality control during substrate preparation, plate sandblasting, adhesive mixing, and curing was essential to ensure uniform interfacial bonding and to prevent premature debonding.

2. Future research should investigate the long-term field performance of steel–CFRP hybrid strengthened floor slabs under actual service and seismic conditions in Kunming, including fatigue, freeze–thaw, humidity, and UV exposure tests, in order to construct a comprehensive durability evaluation system for aged high-rise buildings.

3. Further study should be carried out on the effects of different steel-plate grades, CFRP fibre architectures, and anchorage measures (such as U-shaped CFRP wraps or mechanical end anchors) on the performance of hybrid systems, and on their applicability to two-way and continuous floor slabs under realistic boundary conditions.

4. A comprehensive life-cycle assessment and cost–benefit analysis should be conducted to quantify the economic and environmental advantages of prefabricated steel–CFRP hybrid retrofitting over traditional strengthening methods, and to provide data support for local policy formulation and industrial promotion in the seismic-prone regions of southwestern China.

These future investigations would support the practical implementation of prefabricated steel–CFRP hybrid retrofitting in real building-renovation projects and promote the sustainable upgrading of Kunming's aged high-rise residential stock.

Acknowledgements

The authors would like to express their sincere gratitude to the staff and technicians of the Structural Engineering Laboratory of Kunming University of Science and Technology for their assistance in specimen retrieval, strengthening construction, and loading tests. Appreciation was also extended to Pathumtani University for the academic support, and to the relevant institutions in Kunming for providing access to the decommissioned residential building and

information on local seismic and climatic characteristics. Their contributions were essential to the successful completion of this study.

References

Altemen, A. A. G., Medhlom, M. K., & Özakça, M. (2024). Structural behavior of full-scale novel hybrid layered concrete slabs reinforced with CFRP and steel grids under impact load. Buildings, 14(9), 2625.

Ciampa, E., Ceroni, F., De Angelis, A., & Pecce, M. R. (2023). Bond tests on concrete elements externally bonded with steel plates and assessment of bond strength models. Engineering Structures, 296, 116835.

Fardis, M. N. (2018). Seismic design, assessment and retrofitting of concrete buildings. Springer.

Gong, Y. Z., Kang, S., Liu, M. T., Liang, G. W., & Yang, Y. (2021). Experimental study on flexural behavior of damaged RC slabs strengthened with bonded steel and combination of steel plates and CFRP. Journal of Hunan University (Natural Sciences), 48(3), 65–74.

Han, Z., Qu, W., & Zhu, P. (2023). Research on hybrid FRP–steel-reinforced concrete slabs under blast load. Buildings, 13(4), 1058.

Li, S. C., et al. (2011). Application of CFRP composite in structural reinforcement. Highway Traffic Science and Technology, 28(5), 1–8.

Li, J., et al. (2019). Research on the application of carbon cloth composites in building structure reinforcement. Journal of Architectural Structures, 40(6), 1–12.

Ministry of Housing and Urban-Rural Development of China. (2013). Code for Design of Strengthening of Concrete Structures (GB 50367-2013). China Architecture & Building Press.

Ministry of Housing and Urban-Rural Development of China. (2019). Standard for Test Methods of Concrete Structures (GB/T 50152-2019). China Architecture & Building Press.

Ministry of Housing and Urban-Rural Development of China. (2021). General Code for Appraisal and Strengthening of Existing Buildings (GB 55021-2021). China Architecture & Building Press.

Nguyen, V. S., Nguyen, X. H., Le, D. D., Tran, C. T. N., & Nguyen, A. D. (2025). Experimental studies on torsional behavior of reinforced concrete beams strengthened using hybrid carbon and basalt FRP sheets. Structural Concrete, 26(5), 6594–6618.

Triantafillou, T. C. (2016). Textile fibre composites in civil engineering. Woodhead Publishing.

Wang, L., Zhao, Y., & Chen, M. (2020). Case study on synergistic steel-CFRP strengthening of high-rise building floors in Yunnan Province. Engineering Structures, 225, 111213.

Wu, G., et al. (2021). Interfacial behaviour of steel–CFRP composite strengthened concrete members. Composite Structures, 261, 113568.

Xiao, Y., Zhang, L., & Zhou, F. (2022). Light-weight FRP reinforcement for rapid retrofitting of existing RC structures. Construction and Building Materials, 318, 126038.

Yang, X., et al. (2017). Strengthening of RC columns by external steel jacketing under heavy loads. Engineering Structures, 145, 158–170.

Yu, Q. Q., Gao, B., Xu, H. B., & Gu, X. L. (2025). Experimental study on interfacial bond behavior between CFRP and steel under constant amplitude fatigue loading. Engineering Mechanics. (in press).

Zhang, F. Y., He, B. Z., Wu, Y. X., et al. (2024). Experimental study on flexural behavior of existing stone slabs strengthened by CFRP plate. Engineering Mechanics, 41(12), 138–149.